

Molecular Winston Cone

Adam West

March 29, 2017

1 Introduction

The Winston cone is a non-imaging optical element that is most commonly used to spatially compress light; rays passing into the cone's entrance aperture are internally reflected until exiting through a smaller aperture whereby the spatial distribution is smaller, but the angular distribution of the trajectories is larger (thus conserving phase space density). If we consider rays propagating in the opposite direction, the angular distribution is compressed at the expense of a larger spatial distribution.

If we could apply the same transformation to molecular trajectories we would effectively 'cool' in the transverse direction (no energy is removed so we must also heat in the longitudinal direction). In this document I consider how viable such a process might be. I will say very little about the mechanism for producing the cone.

A nice description of the Winston cone and other non-imaging optics is provided in the book *High Collection Nonimaging Optics* by Welford and Winston. Perhaps the most useful description of the shape is given by Eq. 4.6:

$$(r \cos \theta_m + z \sin \theta_m)^2 + 2r_{\text{in}}(1 + \sin \theta_m)^2 r - 2r_{\text{in}} \cos \theta_m (2 + \sin \theta_m) z - r_{\text{in}}^2 (1 + \sin \theta_m)(3 + \sin \theta_m) = 0 \quad (1)$$

where r is the radial size at a given axial position z , θ_m is the maximum angle that rays can be accepted at if travelling from the large aperture to the small (without being reflected back) — for us this is used to parametrise the cone since all rays going through the small aperture will exit through the large aperture. A smaller θ_m gives a larger cone and more concentration of the angular distribution. r_{in} is the radial size of the small (input) aperture.

One can rewrite this equation as

$$0 = ar^2 + br + c \quad (2)$$

$$a = \cos^2 \theta_m$$

$$b = 2z \cos \theta_m \sin \theta_m + 2r_{\text{in}}(1 + \sin \theta_m)^2$$

$$c = z^2 \sin^2 \theta_m - 2zr_{\text{in}} \cos \theta_m (2 + \sin \theta_m) - r_{\text{in}}^2 (1 + \sin \theta_m)(3 + \sin \theta_m)$$

from which we can solve for r .

$$r = \frac{-(2z \cos \theta_m \sin \theta_m + 2r_{\text{in}}(1 + \sin \theta_m)^2) \pm \sqrt{(2z \cos \theta_m \sin \theta_m + 2r_{\text{in}}(1 + \sin \theta_m)^2)^2 - 4 \cos^2 \theta_m z^2 \sin^2 \theta_m - 2zr_{\text{in}} \cos \theta_m (2 + \sin \theta_m)}}{2 \cos^2 \theta_m} \quad (3)$$

It is also useful to note that the overall length of the cone is given by

$$L = r_{\text{in}}(1 + \sin \theta_m) \cos \theta_m / \sin^2 \theta_m \quad (4)$$

$$= \frac{r_{\text{in}}}{\tan \theta_m} (1 + 1/\sin \theta_m). \quad (5)$$

With this definition of the profile it is a simple matter to implement specular reflection off of it.

2 Trajectory Simulation

Simulation of molecule trajectories proceeds in a manner entirely analogous to that used to simulate e.g. a magnetic lens in ACME. For more details see my other write ups. A schematic of this geometry is given in Fig. 1. To include

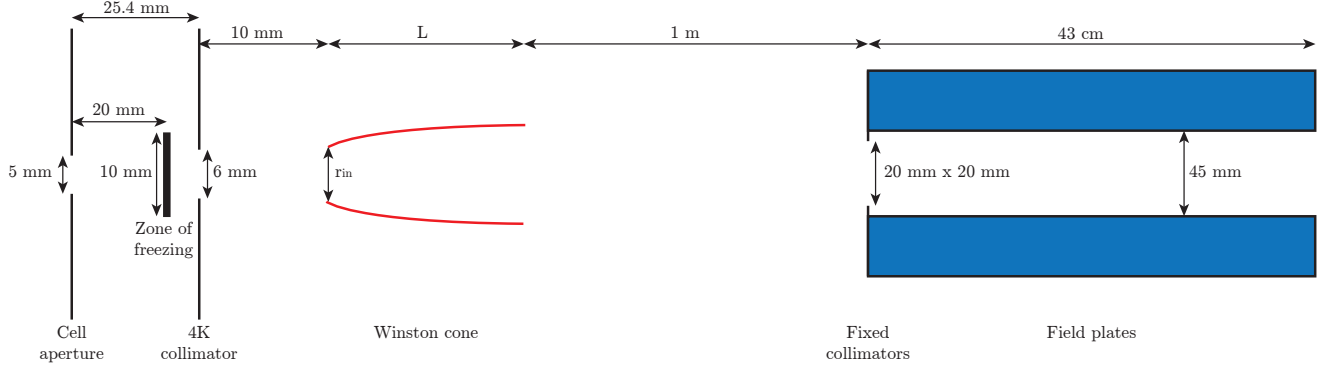


Figure 1: Schematic of the geometry assumed for calculating potential gain afforded by a molecular Winston cone. Not to scale.

a Winston cone I assume that the input (small) aperture is located a distance of 1 cm from the 4 K collimator and has a radius of 5 mm. There is assumed to be a zone of freezing 1 cm in diameter and 2 cm downstream of the cell (5.4 mm upstream of the 4 K collimator). The molecules have a spatially uniform distribution and Gaussianly distributed velocities according to measured beam properties. The molecules are emitted from the zone of freezing, are collimated at the 4 K collimator, collimated again at the Winston cone input aperture, are reflected in the cone, exit and then travel 1 m to the interaction region where they are collimated by the fixed collimators and pass through the field plates. I make no assumptions about the rest of the beam box.

It may be of some use to quickly outline how I set up the ray-tracing inside the Winston cone — the same code could be used for optics ray-tracing, and the same method used for other reflectors with an analytic profile. The only difficult part of the ray-tracing is performing the reflections appropriately. The following formula relates the reflected velocity, \vec{v}_{out} to the incoming velocity \vec{v}_{in} :

$$\vec{v}_{\text{out}} = \vec{v}_{\text{in}} - 2(\vec{v}_{\text{in}} \cdot \hat{n})\hat{n} \quad (6)$$

where \hat{n} is the normal of the surface at the point of reflection. We can calculate \hat{n} using

$$\hat{n} = \frac{\vec{v}_1 \times \vec{v}_2}{|\vec{v}_1 \times \vec{v}_2|} \quad (7)$$

where \vec{v}_1 and \vec{v}_2 are two vectors in the plane of the surface. One of these vectors is trivial — the cylindrical symmetry ensures that an azimuthal vector is always in the plane of the cone, so

$$\vec{v}_1 = \begin{pmatrix} -\sin \phi \\ \cos \phi \\ 0 \end{pmatrix} \quad (8)$$

where the cone axis is along \hat{z} and phi is the azimuthal angle given by $\phi = \tan^{-1}(y/x)$.¹ We can compute \vec{v}_2 as the vector with no azimuthal component. If we describe the radial profile of the cone as $W(z)$, according to Eq. 1, we can write

$$\vec{v}_2 = \begin{pmatrix} (W(z + \delta z) - W(z)) \cos \phi \\ (W(z + \delta z) - W(z)) \sin \phi \\ \delta z \end{pmatrix}. \quad (9)$$

The first two elements describe the change in radius of the cone and get resolved in the x and y directions according to ϕ . The third element is the corresponding z distance over which this change is considered.

The above algebra is applied whenever a particle's radial position exceeds $W(z)$.

¹Use atan2 to get the correct quadrant.

3 Results

As an illustration, Fig. 2 show some example trajectories through a winston cone. The blue circles are used to indicate the profile of the cone. Note that a number of trajectories end before the cone — these are the ones

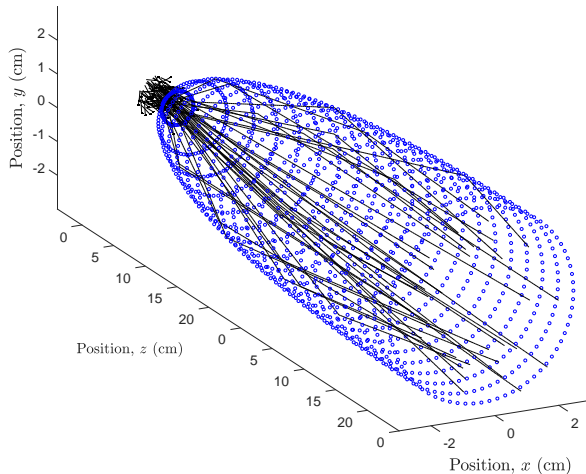


Figure 2: Example trajectories through a Winston cone. The cone’s exit (larger aperture) has a maximum acceptance angle of 10° and a length of around 19 cm.

collimated either by the 4 K collimator or by the cone entrance. You can perhaps convince yourself that the trajectories exiting the cone are better collimated than those entering, but for a clearer picture we can plot the spatial and velocity distributions, shown in Fig. 3. In each plot, individual dots represent a single molecule trajectory. The histograms at the bottom and left are histograms of the scatter plots along the corresponding axes. The heights of the histogram vertical scales are not common.

The top-left figure shows the spatial distributions of the molecules as they enter and exit. The spatial distribution at the input is much denser, and approximately Gaussianly distributed (see histograms). At the exit the distribution is much less dense and has a somewhat counter-intuitive shape. Perhaps most notably, there are quite few molecules near the centre. This can perhaps be understood as follows: molecules exiting at the centre would have to have either passed straight through without reflecting with a very low transverse velocity, which is unlikely, or been reflected at quite a steep angle from the cone, which the cone is specifically designed not to do.

The top-right figure shows the corresponding transverse velocity distribution. As expected in order to conserve phase-space area, the velocity distribution is narrowed by the cone. We also see that the shape of the distribution is not significantly altered. For this particular cone the FWHM of the distribution is approximately halved in both directions.

The bottom-left figure shows a phase space plot for one of the transverse directions. At the input, there is a strong correlation between position and velocity as expected, and again the distributions are approximately Gaussian. At the output, the spatial distribution is no longer Gaussian, reflecting, as in the top-left figure, the fact that this is a non-imaging element. We see that molecules near the centre have a relatively low velocity, suggesting they have simply passed straight through — again the shape of the cone makes it difficult for molecules at the centre to have been reflected. Towards the edges we see that the velocity distribution gets significantly broader.

The bottom-right figure shows the distributions of radial and longitudinal velocity components. We see again that we are compressing the radial velocity, and we know that we must broaden the longitudinal velocity. This is perhaps best seen in the left-hand histograms, but the effect is small since the longitudinal velocity is initially significantly bigger than the transverse velocity.

Hopefully the preceding data have helped to give a little intuition into how the cone works, now we will examine how much it could help us in the experiment. Fig. 4 shows in black the calculated gain in molecule number as a function of the acceptance angle of the cone exit aperture. We see that as the acceptance angle becomes smaller

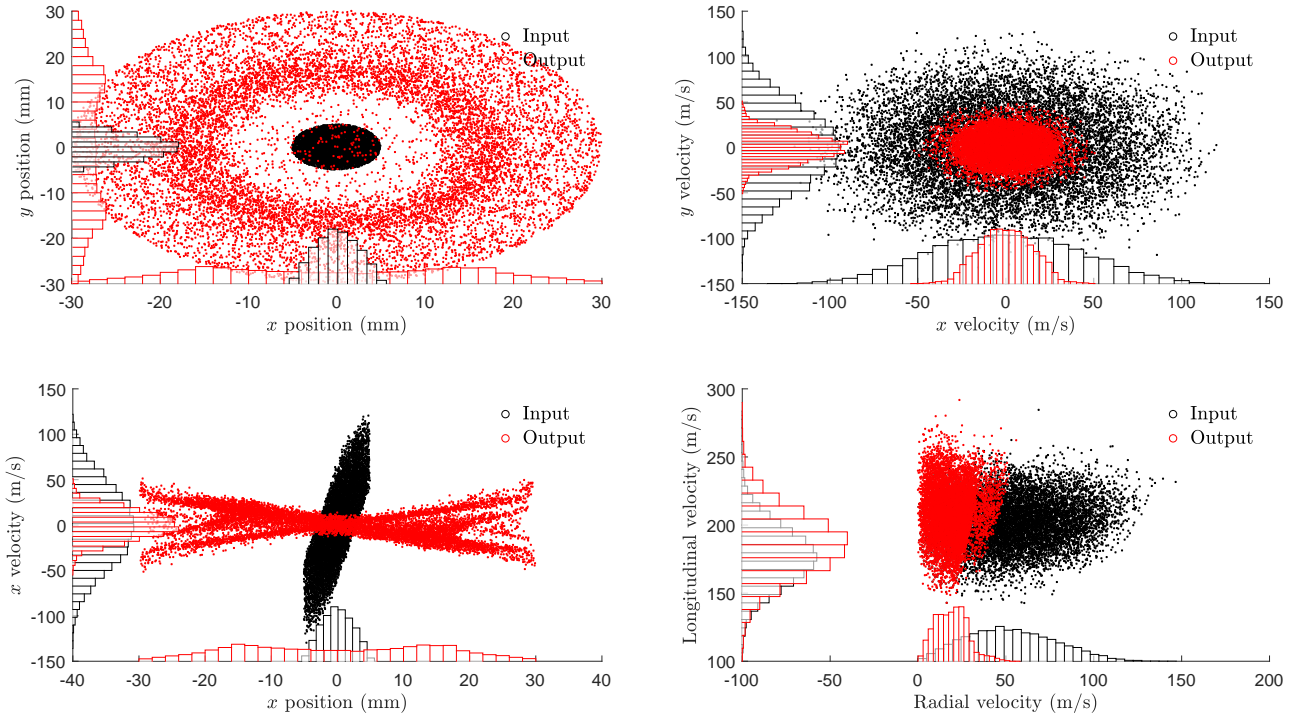


Figure 3: Example spatial and velocity distributions for molecules passing through the Winston cone shown in Fig. 3.

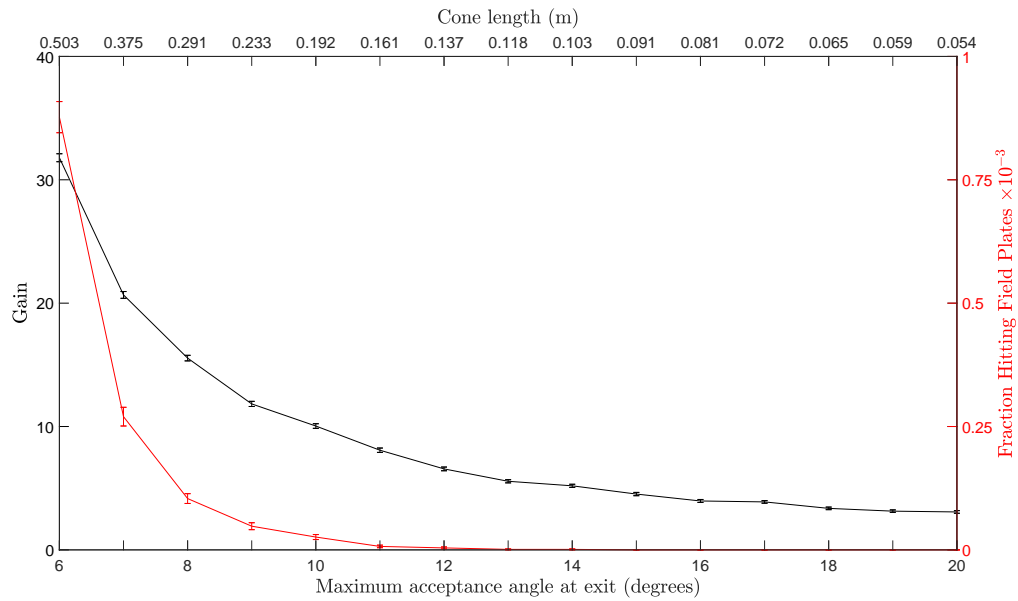


Figure 4: Gain in molecule number (black) and fraction of molecules hitting the field plates (red) as a function of the acceptance angle of the Winston cone's exit aperture.

there is a significant increase in molecule number, with a gain of around a factor of 30 achieved for the smallest angle considered. Unfortunately, whilst the x -axis of this plot is linear in this angle, it is significantly non-linear in cone length; smaller angles require dramatically larger lengths (up to 50 cm in this plot — see top axis). If we aimed for a factor of 10 improvement, however, one would need a length of about 20 cm. Also plotted in red is the fraction of molecules hitting the field plates. It is exactly zero for angles of 15 degrees or more.

We can also consider changing the size of the small aperture of the Winston cone. We find that increasing it affords a small increase in the gain, with an associated further increase in the required cone length. This improvement comes from simply capturing more of the molecules from the source. The plots shown here have an aperture size such that almost all are captured.

4 Required E-Field

In order to assess how feasible this method is, an important consideration is whether we can produce an effective reflective surface. One way to do this would be to use an electric field and the induced Stark shift. Let's assume that we use the $|J = 2, M = 0\rangle$ state of ThO. The corresponding Stark shift is shown in Fig. 5. We see that the

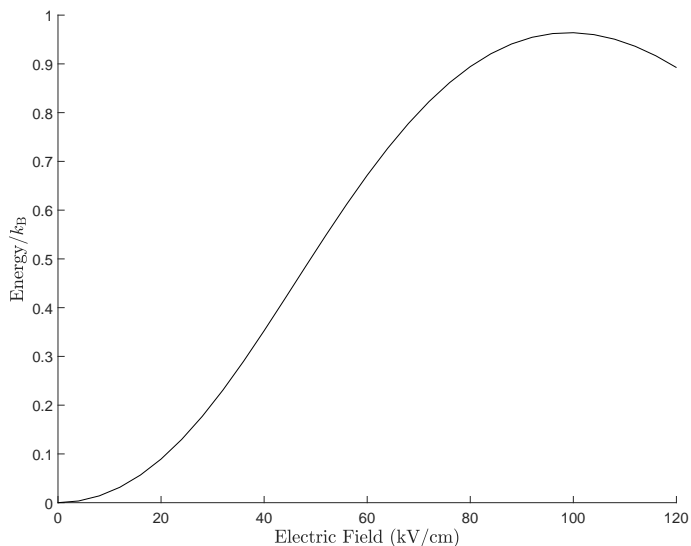


Figure 5: Stark shift for the $|J = 2, M = 0\rangle$ state of ThO.

potential turns over at around 100 kV/cm and the potential depth is around 1 K. It is thus important to check whether this potential depth would be sufficient to reflect the molecules we simulate. This was assessed as follows: Everytime a trajectory was reflected off the cone, the component of the velocity normal to the cone's surface was calculated and stored. If trajectories had multiple reflections, the largest value of this normal component was kept. After trajectories had propagated through the system only the normal velocities at reflection of 'good' molecules were kept. This process was repeated for many iterations of the simulation, collating results. After this, the normal velocity was converted to a kinetic energy, and then divided by k_B . The cumulative distribution of these energies is shown in Fig. 6. We see that the associated energy is very high, significantly higher than the depth of the Stark potential. If we have a potential energy depth of $E/k_B = 1$, then only 0.3% of the successful molecule trajectories would be able to be reflected.

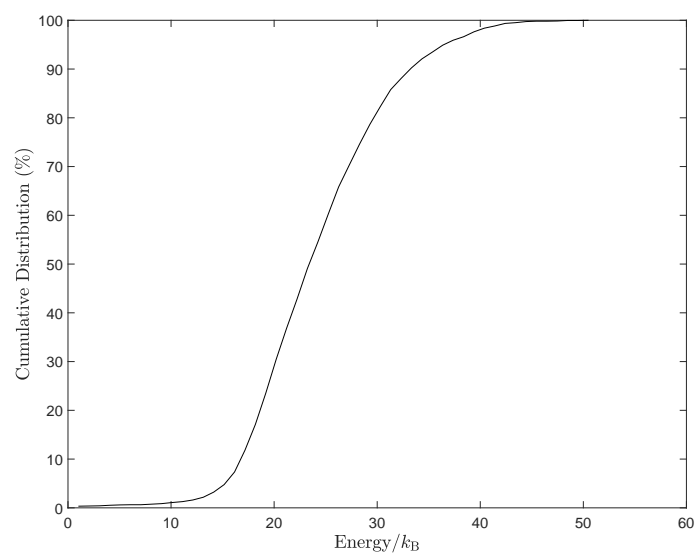


Figure 6: Cumulative distribution of the normal component of velocity at reflection of ‘good’ molecule trajectories, expressed as a kinetic energy.